BOLETIN DE LA SOCIEDAD ESPAÑOLA DE
Cerámica y Vidrio
www.elsevier.es/bsecv

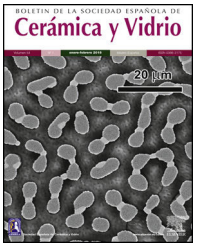


# Antimicrobial properties of different multilayered scaffolds complexed with metronidazole and metronidazole-ozone

*María Rosario Sánchez-Carreño López*[a,*], *Vicente M. Gómez-López*[b], *Maria Teresa Mercader-Ros*[c], *Carmen Lucas-Abellán*[c], *Dennis A. Silva-Cullishpuma*[c], *Pablo Velasquez*[d], *Karina Salazar*[d], *Jose Eduardo Maté Sánchez de Val*[a,*]

[a] *Department of Biomaterials Engineering, Faculty of Health Sciences, UCAM-Universidad Católica San Antonio de Murcia, Campus de los Jerónimos 135, Guadalupe, 30107 Murcia, Spain*
[b] *Green and Innovative Technologies for Food, Environment and Bioengineering Research Group (FEnBeT), Faculty of Pharmacy and Nutrition, UCAM-Universidad Católica San Antonio de Murcia, Campus de los Jerónimos 135, Guadalupe, 30107 Murcia, Spain*
[c] *Nutrition, Food and Health (NAS), Faculty of Pharmacy and Nutrition, Universidad Católica de Murcia (UCAM), Campus de los Jerónimos 135, Guadalupe, 30107 Murcia, Spain*
[d] *Bioengineering Institute, Universidad Miguel Hernández, Avda. Ferrocarril s/n, Elche, Alicante 03202, Spain*

ARTICLE INFO

*Article history:*
Received 21 September 2024
Accepted 10 March 2025
Available online 28 March 2025

*Keywords:*
Biomaterials
Functional coatings
Bioceramics
Osteonecrosis

ABSTRACT

This study compares two different scaffolds (dicalcium silicate – $Ca_2SiO_4$ – core covered with a glass of composition $Ca_2P_6O_{17}$ doped with lithium and with strontium) loaded with metronidazole alone and with metronidazole combined with ozone. Complexes metronidazole-2-hydroxypropyl-β-cyclodextrins (HP-β-CDs) were used to increase the solubility and availability of metronidazole. The concentration of metronidazole used was 40.8 mg/mL (58.4 mM), with a molar ratio of 1:1 and 1.5 mL of ozone oil were added to the different scaffolds. The disk diffusion method against the Gram-positive bacterium *Staphylococcus aureus* and the Gram-negative bacterium *Escherichia coli* showed microbial inhibition but not statistically significant ($p > 0.05$) halo inhibition produced by metronidazole alone and that produced by metronidazole combined with ozone.

This research is expected to have strong social impact directly affecting the quality of life of those affected by osteonecrosis as these nanostructures anchored to structures with a porous 3D-core could facilitate bone regeneration promoted by cell adhesion, vascularization and nutrients supply.



* *Corresponding authors.*
E-mail addresses: mrsanchezcarreno@ucam.edu (M.R. Sánchez-Carreño López), jemate@ucam.edu (J.E. Maté Sánchez de Val).
https://doi.org/10.1016/j.bsecv.2025.03.002

## Propiedades antimicrobianas de diferentes andamios multicapa complejados con metronidazol y metronidazol-ozono

*Palabras clave:*
Biomateriales
Recubrimientos funcionales
Biocerámicas
Osteonecrosis

R E S U M E N

Este estudio compara dos andamios diferentes (núcleo de silicato dicálcico - $Ca_2SiO_4$ - recubierto con un vidrio de composición $Ca_2P_6O_{17}$ dopado con litio y con estroncio) cargados con metronidazol solo y con metronidazol combinado con ozono. Se utilizaron complejos metronidazol-2-hidroxipropil-β-ciclodextrinas (HP-β-CDs) para aumentar la solubilidad y disponibilidad del metronidazol. La concentración de metronidazol utilizada fue de 40.8 mg/mL (58.4 mM), con una relación molar de 1:1 y se agregaron 1.5 mL de aceite de ozono a los diferentes andamios. El método de difusión en disco contra la bacteria Gram positiva *Staphylococcus aureus* y la bacteria Gram negativa *Escherichia coli* mostró inhibición microbiana pero no estadísticamente significativa ($p > 0.05$) entre la inhibición del halo producido por metronidazol solo y el producido por metronidazol combinado con ozono.

Se espera que esta investigación tenga un fuerte impacto social y que afecte directamente a la calidad de vida de los afectados por osteonecrosis, ya que estas nanoestructuras ancladas a estructuras con un núcleo 3D poroso podrían facilitar la regeneración ósea promovida por la adhesión celular, la vascularización y el suministro de nutrientes.



## Introduction

Osteonecrosis is not an specific pathology but the consequence of several conditions leading to bone death due to compromise blood flow and, consequently, oxygen supply [1,2]. Due to the wide range of possible causes of osteonecrosis, as well as the large amount of aging population on treatment with bisphosphonates, it is difficult to obtain epidemiological data worldwide but, for sure, osteonecrosis is a highly prevalent pathology among population. In addition, this pathology seriously affects quality of life of the patients which makes essential to find a predictable treatment.

Common causes of osteonecrosis are infection, steroid use, malformation, tumor resection, and traumatic injuries. Other described causes are alcohol intake, hyperlipidemia, systemic lupus erythematosus, sickle cell disease, Gaucher disease, decompression sickness, acute lymphoblastic leukemia, HIV, idiopathic osteonecrosis, among others [2,3]. In 2003, a new term was reported in the literature, osteonecrosis of the jaw (ONJ) or bisphosphonate-related osteonecrosis of the jaw (BRONJ) as it was usually associated to cancer patients treated with high doses of intravenous bisphosphonates. BRONJ is a rare condition in patients with osteoporosis/other pathologies using bisphosphonates orally but still should be considered the risk [4]. This entity is now known as medication-related osteonecrosis of the jaw (MRONJ) as other types of drugs can also cause osteonecrosis besides bisphosphonates. This entity is defined as exposed bone in the mouth which fails to heal after appropriate intervention over a period of 6 or 8 weeks [5,6]. MRONJ is reported to develop in approximately 8% of the oncology patients taking high-dose of bisphosphonates or denosumab and in 0.01% of osteoporotic patients taking low-dose bisphosphonates or denosumab [7].

Fortunately the bone has the ability to regenerate itself although regeneration conditions are not always ideal, especially in large size bone defects [3,7]. Because of this, to repair osteonecrosis lesions, several materials have been tried over the years, such as autologous and allogenic bone grafts, natural polymers, synthetic polymers, metal, composites and bioceramic and bioglass. All these materials have limitations and, currently, there is no consensus of what the material of choice is [8]. Hydroxyapatite and similar bioceramic materials have been studied in recent years in the bone tissue regeneration field [3,8–16]. Calcium silicate has demonstrated by several authors the capability of inducing hydroxyapatite formation, promoting cell growth, enhancing angiogenesis and osteoinduction [16,17]. Strontium at low (physiological) concentration has been described as beneficial as it can re-establish the imbalanced activity between osteoclasts and osteoblasts, which is the primary cause of osteoporosis [10–12,15,18]. In this particular experiment, 16 multilayered scaffolds have been used, 8 formed by a dicalcium silicate core covered with a glass of composition $Ca_2P_6O_{17}$ doped with lithium and other 8 scaffolds where strontium was added on the surface. These scaffolds were loaded with metronidazole alone and with a combination of metronidazole and ozone to simultaneously treat the infection associated to osteonecrosis lesions. Metronidazole was chosen as it has always been the drug of choice to treat anaerobic infections [19–21]. Ozone was added to half of the scaffolds as it is widely known the bactericidal properties of ozone gas [22–26], but also in other states such as oil, like it was used in this study, or water [27–29]. It seems that addition of ozone can be beneficial against antimicrobial-resistant bacteria [23].

It is already known by the literature the benefit of antibiotic-loaded hydroxyapatite on bony defects is both antimicrobial and reparative. The nanostructured hydroxyapatite allows the loading of antibiotics and a fast biomaterial resorption. Moreover, the hydroxyapatite protects the drug by preventing its diffusion and degradation from body fluids

**Table 1 – Composition (mol%) of the 3D multilayered scaffolds.**

| Sample | $C_2S$-core | | P6-layers | | | Outer layer | | |
|---|---|---|---|---|---|---|---|---|
| | TEOS | $CaCO_3$ | TEP | $CaCO_3$ | $Li_2CO_3$ | TEOS | $CaCO_3$ | $SrCO_3$ |
| $C_2S(2P_6)C_2S$ | 33.33 | 66.66 | 71.73 | 23.91 | 4.34 | 33.33 | 66.66 | – |
| $C_2S(2P_6)C_2S$-Sr | 33.33 | 66.66 | 71.73 | 23.91 | 4.34 | 33.35 | 65.99 | 0.67 |

and/or its retention time in the body. In this way, the loaded drug is used and concentrated locally [7,13,30].

The administration of systemic drugs in conditions such as osteomyelitis poses significant challenges due to the high toxicity of the drugs, which affects not only targeted cells but also all organs of the patient [31,32]. This significantly impacts the patient's quality of life during treatment and may result in serious side effects [33–35]. To address these issues, we propose utilizing developed nanostructures as drug reservoirs, including drugs such as metronidazole or encapsulated ozone, known for their positive effects on tissue regeneration in necrotic lesions and recurrent infections. Furthermore, combining these reservoirs with certain bacteriostatic and antibacterial substances can greatly enhance their effectiveness.

Metronidazole was encapsulated into a cyclodextrin (CD) in order to increase its stability and generate a slow-release since cyclodextrin encapsulation acts as a dosing pump [23]. Furthermore, ozone was also added in half of the scaffolds as it has anti-inflammatory, analgesic, and immunostimulant properties and promotes tissue regeneration [24] besides its bactericidal properties [25–29]. Cyclodextrins are cyclic oligosaccharides composed of bridged glucopyranose subunits, truncated cone-shaped and with a cavity in the center. They have been used mainly in food, pharmaceutical and biological industries due to their inclusion properties for years. The modification used in this study of the β-CD, one of the native types of CD, has the advantage of providing high solubility in water, which is advantageous for future biological applications [27]. In addition, these compounds were produced in a solid state through Spray Drying, a method known to enhance their preservation [36–39], as reported by other researchers [40,41]. This process enhances their stability and viability.

The goal of this research was to test if the encapsulation of metronidazole in β-CDs would achieve an effective antimicrobial concentration and whether the addition of ozone would improve the antimicrobial activity in multilayered scaffolds with and without strontium in the outer layer.

## Materials and method

### *Scaffold preparation*

3D porous ceramic scaffolds were prepared with the sol gel method together with the polymeric replica technique, with 20 ppi DINA4 10 mm sponges (Quality materials). In a first stage, the $C_2S$ (dicalcium silicate – $Ca_2SiO_4$) core was obtained from the commercial chemicals: TEOS (tetraethyl orthosilicate, Aldrich ≥ 98%) and $CaCO_3$ (calcium carbonate, Sigma ≥ 99%). The hydrolysis of the precursor was carried out using hydrochloric acid, obtaining a homogeneous mixture with a pH between 2 and 3. Following that, the polymeric sponge (13 mm diameter and 10 mm long) was submerged from 30 to 40 times and then dried for 15 min at 160–180 °C after each immersion. After that, a heat treatment was applied to the sponge heating it up to 1050 °C for 8 h.

In a second stage (P6), the core was coated with a glass phase from the reagents triethyl phosphate (TEP) (Aldrich triethyl phosphate ≥ 99.8%), $CaCO_3$ (calcium carbonate, Sigma ≥ 99%) and $Li_2CO_3$ (lithium carbonate, Sigma–Aldrich 99.8 ≥ %). The hydrolysis of the reagents was carried out using hydrochloric acid, keeping the mixture at a pH between 4 and 5. In this case, the previously prepared $C_2S$ core was immersed ten times in the new solution described, drying at 140–160 °C for 10 min after each immersion. After this, a heat treatment at 1050 °C for 8 h was carried out. In order to improve mechanical resistance, this vitrification process was done twice.

As a last treatment, to improve cell adhesion, the surface of the 3D multilayered scaffolds was modified using a layer of $C_2S$ doped with 1% $Sr^{+2}$. This was prepared with TEOS, $CaCO_3$ and $SrCO_3$ (strontium carbonate Alfa Aesar 99%). The scaffolds were coated ten times, dried for 20 min at 160–180 °C after each immersion, and finally heat treated at 1050 °C for 8 h. The composition and label of the 3D multilayered scaffolds is found in Table 1.

### *Complexation of metronidazole with 2-hydroxypropyl-β-cyclodextrins*

*Complexation method by aqueous solubility*

The solubility studies of metronidazole, in the presence of 2-hydroxypropyl-β-cyclodextrins (HP-β-CDs), were carried out according to Higuchi and Connors' method [30]. For this, aqueous solutions of increasing concentrations of HP-β-CDs, up to a concentration of 100 mM for HP-β-CDs, in a total volume of 5 mL.

A saturating amount of metronidazole was added to each of the solutions and they were kept in an ultrasonic bath for 90 min, at 20 °C, until equilibrium was reached. Afterwards, the solutions were filtered through a 0.45 μm cellulose acetate filter to eliminate the excess of antibiotic (not dissolved).

The concentrations of dissolved metronidazole in each sample were calculated by measuring their absorbance with a spectrophotometer and using the Lambert–Beer law. This allowed precise determination of the amount of antibiotic dissolved in each solution.

To quantify the amount of metronidazole dissolved in each filtrate, the antibiotic-cyclodextrin complexes were broken by adding 80% ethanol (Scharlau). Subsequently, each of the solutions was introduced into the spectrophotometer, measuring its absorbance at the wavelength of maximum absorption of

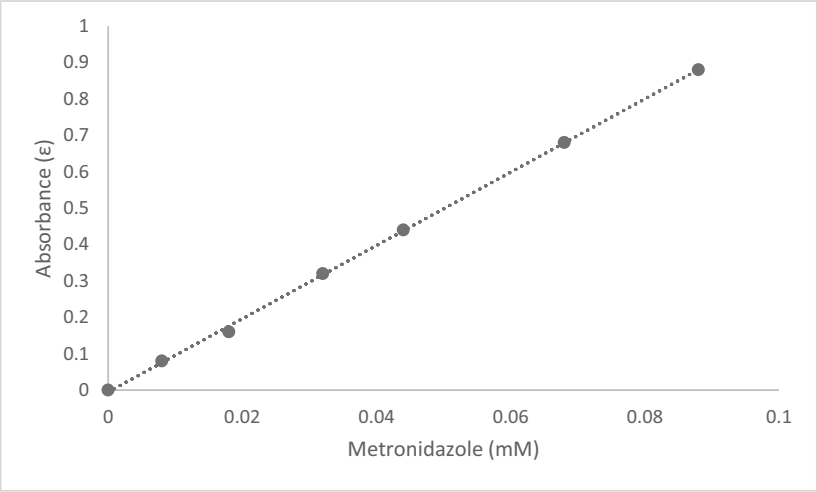


**Fig. 1 – Metronidazole standard calibration curve: calculation of the molar extinction coefficient of metronidazole at 80% ethanol at its maximum absorbance 320 nm (9.9264 $M^{-1}$ $cm^{-1}$).**

metronidazole (320 nm). The concentration of the antibiotic in each solution was determined using the Lambert–Beer law: $A = \varepsilon lc$; (where A is absorbance; $\varepsilon$, molar extinction coefficient; l, path length (10 mm); and c, concentration of sample in nM), calculating the molar extinction coefficients at 80% ethanol and metronidazole (Fig. 1).

The apparent stability constant ($K_C$) value of metronidazole and HP-β-CDs was calculated from the solubility studies using the following equation [30]:

$$K_C = \frac{\text{slope}}{S_0(1 - \text{slope})}, \quad [1]$$

where $S_0$ is the solubility of metronidazole in the medium and "slope" is the slope of the straight line obtained in the solubility study for each of them.

The complexation efficiency (CE) of each scaffold was calculated using the following equation [42]:

$$CE = \frac{[\text{Metronidazole} - \text{CD}]}{[\text{CD}]t} = S_0 \cdot K_c. \quad [2]$$

For data analysis, the concentration of total metronidazole was represented against the concentration of HP-β-CDs.

*Microwave irradiation method*

To increase the concentration of metronidazole in the solution, this study was carried out using the microwave irradiation method. Firstly, three aqueous solutions of 20 mM of HP-β-CDs in 150 mL were prepared and irradiated with microwaves (LG Grill Wavedom, LG Electronics, Madrid, Spain) at 700 W for 30 s, at 10 s intervals, until reaching a temperature of 70 °C in the solution. The metronidazole was then added to each solution and irradiated again for 30 s at 10 s intervals, until reaching 70 °C. Subsequently, the samples were shaken and kept for 12 h in sealed vials in the dark. Next, following the procedure described above, the samples were irradiated again, until reaching 70 °C.

To quantify the amount of metronidazole dissolved before atomization, the antibiotic-CD complexes were broken by adding 80% ethanol. Sample analysis was performed on an Agilent 1200 series HPLC (high-performance liquid chromatography) equipment, formed by a quaternary pump, a degasser, an autosampler with thermostat, a column compartment, and a DAD (Diodo Array Detector). Additionally, a reverse phase column is used: LiChrospher® 100 RP-18 (250 mm × 4 mm ID, 5 μm particle size). For the analysis, a column temperature of 30 °C is defined, an injection volume with water wash of 20 μL and a flow rate of 1 mL/min. The mobile phase is composed of A: 1% acetic acid and B: acetonitrile and the total gradient time is 20 min. Initially, 20% B is maintained for 5 min, then a ramp is made until reaching 50% B at 10 min. Immediately after B is reduced to 20% until 15 min and maintained 20% B until 20 min. Finally, the results were processed using Agilent ChemStation software.

The standard calibration curve was carried out by analyzing samples with seven different concentrations of metronidazole in triplicates with the previously described method.

The standard calibration curve showed good linearity in the concentration range of 0.001–0.5 mg/mL of metronidazole, obtaining a linear regression coefficient > 0.999, indicating a high degree of linearity (Fig. 2).

The solutions prepared by the microwave irradiation method were atomized to convert the complexes into powder. This process was carried out using a laboratory-scale atomizer, Mini Spray Dryer Büchi B290 (Flawil, Switzerland). The operating conditions of the drying process were: air inlet temperature 180 °C, 2 °C, air outlet temperature 70 °C, flow rate of 5 mL/min, air pressure 3.2 bar, and nozzle diameter of 1.5 mm [36]. Once the powder is obtained, it is collected and stored at room temperature (25 °C) until its use.

Precipitation was controlled in order to prevent large particles from blocking the vaporization device or the nozzle [43].

The process yield (PY) was determined gravimetrically, as the relationship between the grams obtained after spray

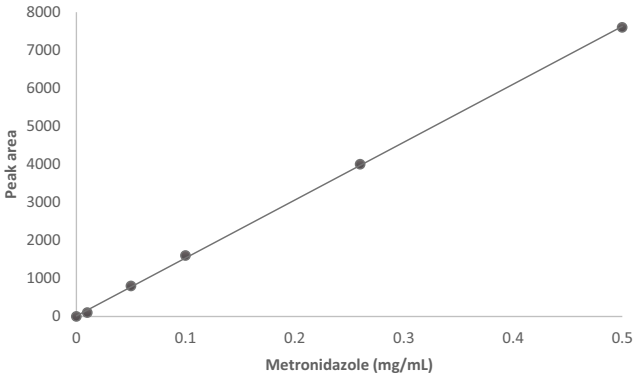


**Fig. 2 – Standard calibration curve for metronidazole for HPLC determinations.**

drying and the amount of solids contained in the solution according to Di Battista et al. [44]:

$$\text{PY\%} = \frac{\text{mass of powder collected}}{\text{mass of solids in solution}} \times 100. \quad [3]$$

The encapsulation efficiency (EE) measures the proportion of metronidazole in the powder in relation to the total content, it was calculated according to Frascareli et al. [45]:

$$\text{EE}\,(\%) = \frac{\text{Metronidazole after atomization}}{\text{Metronidazol before drying by atomization}} \times 100. \quad [4]$$

The total content of encapsulated metronidazole was calculated according to the following formula:

$$\text{Loading}\,(\%) = \frac{\text{Encapsulated Active Material}}{\text{Total powder obtained}} \times 100. \quad [5]$$

*Functionalization of metronidazole-encapsulated scaffolds*

First, the scaffolds were selected to be more or less the same size and weighed on a precision balance. The average size of the scaffolds was 11.38 mm × 11.38 mm × 9.44 mm and the average weight, 585.35 mg.

In this study, the scaffolds were tested in order to determine which of them were loaded with the greatest amount of metronidazole.

To load the scaffolds, 1.5 mL of metronidazole-CD complex (58.4 mM of metronidazole in 20 mM of CDs) was added to a Falcon tube where the scaffold was completely covered. This study was carried out in triplicates. Subsequently, the samples were placed in a glass vacuum desiccator and the vacuum pump was kept turned on for 5 min. Then, the pump was turned off and left in place for 10 more minutes. Afterwards, the concentration of metronidazole that remains in the leftover liquid was measured. The scaffolds were put in the oven for 24 h at 40 °C to eliminate any moisture.

To know the concentration of metronidazole that remains in the scaffolds, they were crushed and 1.5 mL of 80% ethanol was added to break up the complexes.

*Ozone addition to the scaffolds with metronidazole*

Ozosana® ozone oil was added to the previously loaded with metronidazole scaffolds to determine if there was more antimicrobial action that with metronidazole alone. The composition of this ozone oil is ozonized helianthus annuus seed oil, ozonized olea europaea oil, mentha piperita oil, tocopherol, tocopheryl acetate and limonene.

The scaffolds were placed in a falcon tube and 1.5 mL of ozone oil were added, covering the whole sample. The study was carried out in triplicates. Subsequently, the samples were placed in a glass vacuum desiccator and the vacuum pump was kept turned on for 5 min. Then, the pump was turned off and left in place for 10 more minutes. After that time, the scaffolds were removed from the leftover oil and left at room temperature for 24 h.

*Antibacterial effect*

The antimicrobial activities of metronidazole alone and metronidazole combined with ozone loaded in both types of scaffolds described were tested using the Gram-negative strain, *Escherichia coli* (CECT 101) and the Gram-positive strain *Staphylococcus aureus* (CECT 239), both from the Spanish Type Culture Collection (CECT), Valencia, Spain. Freeze-dried bacteria were activated by culturing in Nutrient Broth from the CECT activation kit and grown at 37 °C for 24 h, followed by two 10 mL consecutive cultures in Nutrient Broth (Scharlau, Barcelona, Spain).

*Disk diffusion method*

The strains from the second culture were independently spread using a sterile bent rod on a Standard Methods Agar (Panreac, Barcelona, Spain) culture plate. After 15 min, the scaffolds were placed in the center of the agar and incubated at 37 °C for 24 h. A mixture of two antibiotics, penicillin and streptomycin (Capricorn Scientific, Germany) (10 μL) was used as positive control. After incubation time, inhibition zones were measured using an automatic Interscience scan 500 zone reader (Saint-Nom-la-Bretèche, France).

*Statistical analysis*

Data for each strain was analyzed by two-way ANOVA (scaffold and antimicrobial) using IBM SPSS Statistics 27.0 with $p < 0.05$. All samples were run in quadruplicates for both species.

## Results and discussion

The results obtained in this study were as follows.

*Complexation of metronidazole in HP-β-CDs*

*Complexation method by aqueous solubility*

The results obtained in this study indicate that the solubility of metronidazole is significantly increased in the presence of 2-hydroxypropyl-β-cyclodextrins (HP-β-CDs).

For data analysis, the total concentration of metronidazole was graphically represented against the concentration of HP-β-CDs (Fig. 3). This representation revealed a linear

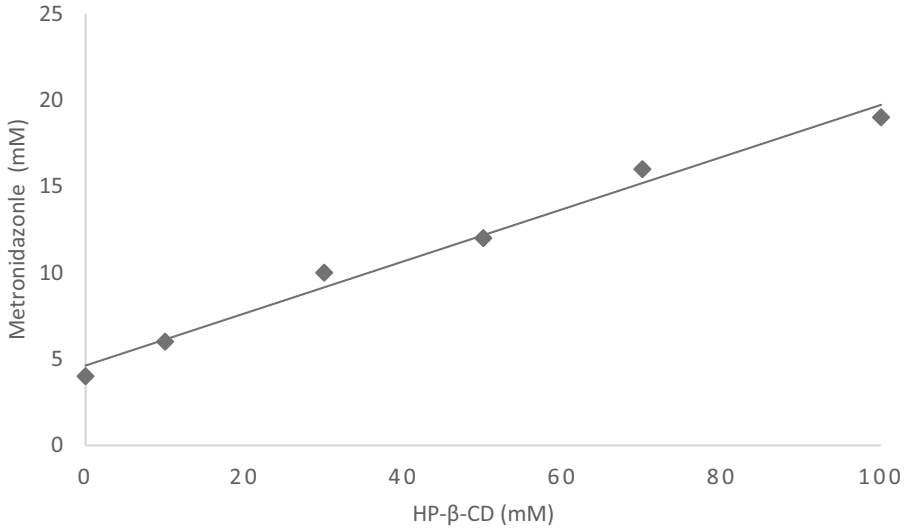


**Fig. 3 – Solubility study of metronidazole-HP-β-CDs.**

**Table 2 – Metronidazole/HP-β-CD complexation constants.**

| Slope | $S_0$ | $K_c$ | CE | Molar ratio |
|---|---|---|---|---|
| 0.1479 | 4.47 nM | 38.83 $M^{-1}$ | 17.8% | 1:6 |

relationship between the concentration of metronidazole in solution and the concentration of HP-β-CDs in the medium. This linear relationship suggests that the stoichiometry of the inclusion complexes formed between metronidazole and HP-β-CDs is 1:1, meaning that each molecule of metronidazole associates with one molecule of HP-β-CD. This finding is aligned with the work of Reichenberg and Rübsamen, who observed a 1:1 stoichiometric ratio in their studies on cyclodextrin-drug complexes [41].

In terms of solubility, it was observed that in the absence of HP-β-CDs, the solubility of metronidazole in water was 4.47 mM. However, by adding HP-β-CDs and increasing their concentration to 100 mM, the solubility of metronidazole in water significantly increased, reaching 19.3 mM (Fig. 3). This represents an almost fivefold increase in the solubility of metronidazole. This is comparable to the results reported by Khan et al., who also documented significant solubility enhancements using CDs for various drugs [31].

This finding is consistent with previous studies that have shown the ability of CDs to improve the solubility of hydrophobic drugs. For instance, Pitha and Koenig and Hedges and Charles have reported similar improvements in drug solubility when using CDs, reinforcing the validity of our results [34,35].

The calculation of the complexation constants and the aqueous solubility limit of metronidazole allowed to calculate the complexation efficiency (CE) (Table 2).

When carrying out CDs saturation studies, it is important to calculate the complexation efficiency (CE) as this value considers, in addition to $K_C$, the aqueous solubility of the encapsulated compound ($S_0$). The results shown in Table 2 confirm that metronidazole complexed with HP-β-CDs in aqueous medium, thus increasing its solubility. This result is crucial for determining the practicality of using these complexes in pharmaceutical applications. Lee et al. emphasized the importance of complexation efficiency in predicting the performance of cyclodextrin-based drug delivery systems [37].

*Microwave irradiation method*

Since the concentration of metronidazole complexed using the phase diagram method with sonication was low (8 mM of metronidazole in 20 mM of CDs) and insufficient to achieve the desired antimicrobial effect when loading the scaffold with the antibiotic, an alternative method was studied. Encapsulation with cyclodextrins *via* microwave irradiation was explored. In this case, the concentration of complexed metronidazole was 8 times higher than that achieved with the phase diagram method (58.4 mM in 20 mM of CDs). Therefore, the microwave irradiation method was chosen to complex metronidazole, allowing the scaffolds to be loaded with the antibiotic at a higher and more effective concentration.

Once the metronidazole has been encapsulated in HP-β-CDs, the concentration to be used in the scaffolds was then decided. CDs, being sugars, can act as a substrate for the bacteria present in the mouth, so it was chosen not to exceed a concentration of 20 mM of HP-β-CDs to avoid bacterial growth. This highlights the practical considerations considered in formulation development. This precaution aligns with findings from Davis et al., who noted similar constraints in using CDs in biological environments [38]. The concentration of metronidazole chosen was 40.8 mg/mL (58.4 mM), with a molar ratio of 1:1. To increase the concentration of metronidazole in the solution, this study was carried out using the microwave irradiation method, since it is a method that has shown better results in obtaining solid complexes [43,46]. The analysis of the samples was carried out on HPLC equipment, as described in materials and method.

Once the complexation of metronidazole with HP-b-CDs was determined using the microwave irradiation method, the sample was subjected to atomization. The results obtained for atomization yield were as follows:

- Process yield (PY) was 56%. This result was within the expected range, as our experience suggests that the usual yield falls between 50% and 60% as suggested by Vázquez and Martín [39].
- In terms of encapsulation efficiency (EE), values of 90.6% were achieved. These values indicate a high efficiency in the encapsulation process and provide clear information about the amount of metronidazole present in the complex. The high encapsulation efficiency suggests that a significant proportion of the metronidazole has been effectively incorporated into the CD complex, which is crucial for ensuring that the drug is available in the desired form and in the required amounts for its medical applications.
- In terms of encapsulation efficiency (EE) and the content of complexed metronidazole (CM) in the atomized powder, values of 90.6% and 39.7% were achieved, respectively. These values indicate high efficiency in the encapsulation process and provide clear information about the amount of metronidazole present in the complex.

### *Functionalization of metronidazole-encapsulated scaffolds*

Once the concentration of metronidazole encapsulated in CDs was established, the scaffolds were loaded with 1.5 mL (containing 58.4 mM in 20 mM of CDs).

As shown in Table 3, the amount of metronidazole incorporated into the scaffolds ranges from 20% to 21% of the total metronidazole complexed with HP-β-CDs in the initial solution in which the scaffolds are immersed (1.5 mL containing 58.4 mM in 20 mM of CDs). The $C_2S(2P_6)C_2S$-Sr scaffolds achieved the highest fixation yield of the complexed metronidazole, reaching 21% of metronidazole.

**Table 3 – % of metronidazole loaded in the different types of scaffolds.**

| Scaffold | % metronidazole |
|---|---|
| $C_2S(2P_6)C_2S$ | 21 |
| $C_2S(2P_6)C_2S$-Sr | 20 |

Due to the lack of irrigation in the necrotic bone the use of systemic antibiotics does not seem to be beneficial [47], therefore scaffolds loaded with antimicrobials can be a manner of reducing the bacterial load of the lesions. It would be interesting to compare the effectiveness of different antimicrobials in the bacterial reduction, such as doxycycline according to some other studies [7], as well as the bone volume density obtained with different drugs. Further experiments are required against different species usually found in osteonecrosis lesions such as *Porphyromonas*, *Tannerella*, *Prevotella*, *Aggregatibacter*, *Treponema*, among others, and testing different antimicrobials to select the most effective [48] and to determine if the association of ozone to antimicrobials makes a significant difference.

The addition of ozone not only shall be tested for antimicrobial properties but also, in the future, should be tested for *in vivo* bone regeneration as this seems to reduce the hardness of the scaffolds facilitating the formation of new bone [49]. In addition, in patients with osteonecrosis of the femoral head, the treatment with ozone showed a significant decrease in

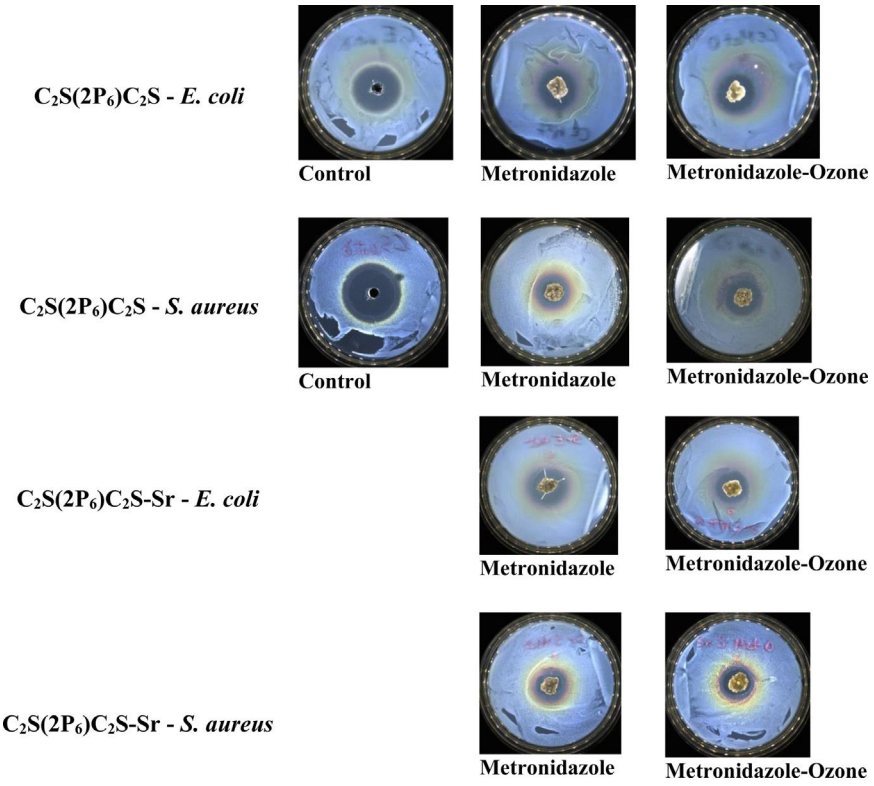


**Fig. 4 – Control with antibiotics and *S. aureus* and *E. coli*. One image per sample of different scaffold type and medication loaded shown: $C_2S(2P_6)C_2S$ inoculated with *E. coli*, $C_2S(2P_6)C_2S$ inoculated with *S. aureus*; $C_2S(2P_6)C_2S$-Sr inoculated with *E. coli*; $C_2S(2P_6)C_2S$-Sr inoculated with *S. aureus*.**

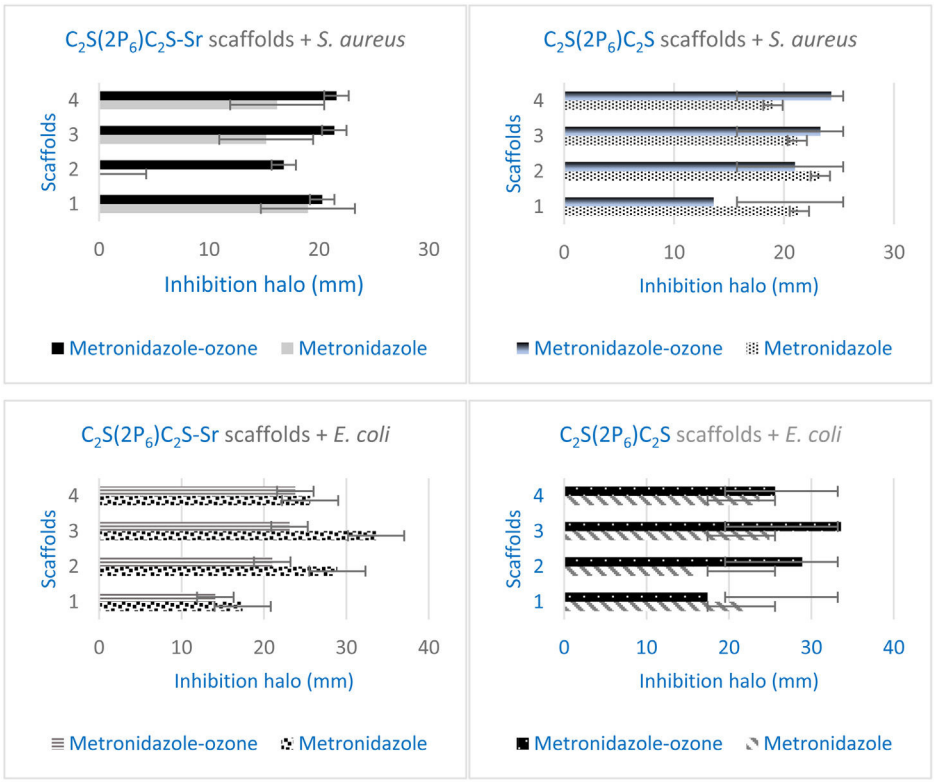


**Fig. 5 – Comparison of the halo measurements in quadruplicates against *S. aureus* and *E. coli* in $C_2S(2P_6)C_2S$ and $C_2S(2P_6)C_2S$-Sr scaffolds loaded with metronidazole only and metronidazole combined with ozone. Error bars mean standard deviation.**

bone marrow edema and it also has been seen that ozone therapy may restore immunological parameters to normal levels [50]. Also, good results were obtained clinically in patients with BRONJ treated with debridement with Piezoelectric surgery and ozone/oxygen therapy [51].

### *Antibacterial effect*

The disk diffusion susceptibility test showed that metronidazole alone and metronidazole combined with ozone had antimicrobial effect when loaded in both types of scaffolds (see Fig. 4) as it was seen in other studies by Kida et al. or Samson et al. [38,52]. This suggests the indication of antimicrobial loaded scaffolds as a topical treatment for osteonecrosis lesions as an alternative to systemic antibiotherapy. The data obtained from the inhibition halos shows no statistical differences ($p > 0.05$) for scaffold type nor for antimicrobial (Fig. 5).

Representative images of the inhibition halo in the different scaffolds can be seen in Fig. 4. Note the halo is irregular due to the shape of the samples and the uneven contact with the surface of the agar.

## Conclusions

The results indicate that the methodology used for encapsulating metronidazole in HP-β-CD scaffolds has been highly effective, providing a product with high encapsulation efficiency and adequate metronidazole content for medical treatment. This underscores the potential of these encapsulation systems in improving the bioavailability and efficacy of metronidazole for various therapeutic applications. These scaffolds will also be tested for cell proliferation.

Although further research, *in vitro* and *in vivo*, is required, it seems that the addition of antimicrobials in $C_2S(2P_6)C_2S$ and $C_2S(2P_6)C_2S$-Sr scaffolds for the regeneration of osteonecrosis lesions can overrun the systemic administration of antibiotics.

In this particular experiment, there was no significant difference with the addition of ozone to metronidazole in any type of scaffold ($p > 0.05$). *In vivo* experiments are required to check if the addition of ozone benefits the mechanical properties of $C_2S(2P_6)C_2S$ and $C_2S(2P_6)C_2S$-Sr scaffolds as the literature suggests. Attending to the type of scaffold, $C_2S(2P_6)C_2S$ ones showed a larger inhibition halo against *S. aureus*, although with hardly any difference when loaded with metronidazole-ozone, while against *E. coli*, $C_2S(2P_6)C_2S$-Sr scaffolds loaded with metronidazole showed, on average, larger inhibition halo, while $C_2S(2P_6)C_2S$ scaffolds loaded with metronidazole-ozone were superior on average. These differences were no statistically significant ($p > 0.05$).

## Funding

This work is part of the project PID2020-116693RB-C21 and PID2020-116693RB-C22, funded by MCIN/AEI/10.13039/501100011033 Spain.

## Conflict of interest

The authors of this article declare that they have no conflict of interest.

## REFERENCES


[1] K. Pavelka, Osteonecrosis, Best Pract. Res. Clin. Rheumatol. 14 (2) (2000) 399–414, http://dx.doi.org/10.1053/berh.2000.0072.

[2] B.S. George Gary, M.M.D. Lane Joseph, Osteonecrosis of the femoral head, JAAOS Global Res. Rev. 6 (5) (2022), http://dx.doi.org/10.5435/JAAOSGlobal-D-21-00176, e21.00176.

[3] M. Laubach, F. Hildebrand, S. Suresh, M. Wagels, P. Kobbe, F. Gilbert, et al., The concept of scaffold-guided bone regeneration for the treatment of long bone defects: current clinical application and future perspective, J. Funct. Biomater. 14 (7) (2023) 341, http://dx.doi.org/10.3390/jfb14070341.

[4] L.H. Ferreira Jr., K.D. Mendonça Jr., J. Chaves De Souza, D.C. Soares Dos Reis, C. Do Carmo Faleiros Veloso Guedes, L. De Souza Castro Filice, et al. Bisphosphonate-associated osteonecrosis of the jaw. Minerva Dent. Oral Sci. https://doi.org/10.23736/S2724-6329.20.04306-X.

[5] I.R. Reid, T. Cundy, Osteonecrosis of the jaw, Skelet. Radiol. 38 (1) (2009) 5–9, http://dx.doi.org/10.1007/s00256-008-0549-x.

[6] M. Kawahara, S. Kuroshima, T. Sawase, Clinical considerations for medication-related osteonecrosis of the jaw: a comprehensive literature review, Int. J. Implant Dent. 7 (1) (2021) 47, http://dx.doi.org/10.1186/s40729-021-00323-0.

[7] R. Sacco, S.C. Sartoretto, R.F. de Brito Resende, J. de Albuquerque Calasans-Maia, A.M. Rossi, V.H. de Souza Lima, et al., The use of hydroxyapatite loaded with doxycycline (HADOX) in dentoalveolar surgery as a risk-reduction therapeutic protocol in subjects treated with different bisphosphonate dosages, Medicina (Kaunas) 59 (1) (2022) 46, http://dx.doi.org/10.3390/medicina59010046.

[8] F. Schulze, A. Lang, J. Schoon, G.I. Wassilew, J. Reichert, Scaffold guided bone regeneration for the treatment of large segmental defects in long bones, Biomedicines 11 (2) (2023) 325, http://dx.doi.org/10.3390/biomedicines11020325.

[9] S. Soleymani, S.M. Naghib, 3D and 4D printing hydroxyapatite-based scaffolds for bone tissue engineering and regeneration, Heliyon 9 (9) (2023) e19363, http://dx.doi.org/10.1016/j.heliyon.2023.e19363.

[10] R. Zhao, S. Chen, W. Zhao, L. Yang, B. Yuan, V.S. Ioan, et al., A bioceramic Scaffold composed of strontium-doped three-dimensional hydroxyapatite whiskers for enhanced bone regeneration in osteoporotic defects, Theranostics 10 (4) (2020) 1572–1589, http://dx.doi.org/10.7150/thno.40103.

[11] T. Zhu, Y. Cui, M. Zhang, D. Zhao, G. Liu, J. Ding, Engineered three-dimensional scaffolds for enhanced bone regeneration in osteonecrosis, Bioact. Mater. 5 (3) (2020) 584–601, http://dx.doi.org/10.1016/j.bioactmat.2020.04.008.

[12] P. Dec, A. Modrzejewski, A. Pawlik, Existing and novel biomaterials for bone tissue engineering, Int. J. Mol. Sci. 24 (1) (2022) 529, http://dx.doi.org/10.3390/ijms24010529.

[13] M. Bordone, A. Bettencourt, Management of bone diseases: looking at scaffold-based strategies for drug delivery, Drug Deliv. Transl. Res. 13 (1) (2023) 79–104, http://dx.doi.org/10.1007/s13346-022-01191-w.

[14] H.F. Pereira, I.F. Cengiz, F.S. Silva, R.L. Reis, J.M. Oliveira, Scaffolds and coatings for bone regeneration, J. Mater. Sci. Mater. Med. 31 (3) (2020) 27, http://dx.doi.org/10.1007/s10856-020-06364-y.

[15] C. Bussola Tovani, T. Divoux, S. Manneville, T. Azaïs, G. Laurent, M. De Frutos, et al., Strontium-driven physiological to pathological transition of bone-like architecture: a dose-dependent investigation, Acta Biomater. 169 (2023) 579–588, http://dx.doi.org/10.1016/j.actbio.2023.07.043.

[16] Y. Ma, B. Zhang, H. Sun, D. Liu, Y. Zhu, Q. Zhu, et al., The dual effect of 3D-printed biological scaffolds composed of diverse biomaterials in the treatment of bone tumors, Int. J. Nanomed. 18 (2023) 293–305, http://dx.doi.org/10.2147/IJN.S390500.

[17] T. Li, M. Peng, Z. Yang, X. Zhou, Y. Deng, C. Jiang, et al., 3D-printed IFN-γ-loading calcium silicate-β-tricalcium phosphate scaffold sequentially activates M1 and M2 polarization of macrophages to promote vascularization of tissue engineering bone, Acta Biomater. 71 (2018) 96–107, http://dx.doi.org/10.1016/j.actbio.2018.03.012.

[18] R.G. Ribas, V.M. Schatkoski, T.L.D.A. Montanheiro, B.R.C. De Menezes, C. Stegemann, D.M.G. Leite, et al., Current advances in bone tissue engineering concerning ceramic and bioglass scaffolds: a review, Ceram. Int. 45 (17) (2019) 21051–21061, http://dx.doi.org/10.1016/j.ceramint.2019.07.096.

[19] S. Löfmark, C. Edlund, C.E. Nord, Metronidazole is still the drug of choice for treatment of anaerobic infections, Clin. Infect. Dis. 50 (s1) (2010) S16–S23, http://dx.doi.org/10.1086/647939.

[20] X. Ji, S. Pushalkar, Y. Li, R. Glickman, K. Fleisher, D. Saxena, Antibiotic effects on bacterial profile in osteonecrosis of the jaw, Oral Dis. 18 (1) (2012) 85–95, http://dx.doi.org/10.1111/j.1601-0825.2011.01848.x.

[21] B. Lončar Brzak, L. Horvat Aleksijević, E. Vindiš, I. Kordić, M. Granić, D. Vidović Juras, et al., Osteonecrosis of the jaw, Dent. J. (Basel) 11 (1) (2023) 23, http://dx.doi.org/10.3390/dj11010023.

[22] R. Morishita, S. Itoh, M. Takeda-Morishita, Evaluation of bactericidal effects of $H_2$- and $O_3$-filled ultrafine bubbles water, Biocontrol Sci. 27 (3) (2022) 139–142, http://dx.doi.org/10.4265/bio.27.139.

[23] A. Roth, A. Krishnakumar, R.R. McCain, M.K. Maruthamuthu, M. McIntosh, Y.X. Chen, et al., Biocompatibility and safety assessment of combined topical ozone and antibiotics for treatment of infected wounds, ACS Biomater. Sci. Eng. 9 (6) (2023) 3606–3617, http://dx.doi.org/10.1021/acsbiomaterials.2c01548.

[24] E. Haddad, M. Pagès, F. Violleau, O. Marsan, M.H. Manero, R. Richard, et al., Ozonized 2-hydroxypropyl-β-cyclodextrins as novel materials with oxidative and bactericidal properties, Carbohydr. Polym. 291 (2022) 119516, http://dx.doi.org/10.1016/j.carbpol.2022.119516.

[25] K. Rangel, F.O. Cabral, G.C. Lechuga, J.P.R.S. Carvalho, M.H.S. Villas-Bôas, V. Midlej, et al., Potent activity of a high concentration of chemical ozone against antibiotic-resistant bacteria, Molecules 27 (13) (2022) 3998, http://dx.doi.org/10.3390/molecules27133998.

[26] N. Smith, A. Wilson, J. Gandhi, S. Vatsia, S. Khan, Ozone therapy: an overview of pharmacodynamics, current research, and clinical utility, Med. Gas Res. 7 (3) (2017) 212, http://dx.doi.org/10.4103/2045-9912.215752.

[27] F. Passidomo, F. Pignatelli, G. Addabbo, C. Costagliola, Topical liposomal ozonated oil in complicated corneal disease: a report on three clinical cases, Int. Med. Case Rep. J. 14 (2021) 327–332, http://dx.doi.org/10.2147/IMCRJ.S311839.

[28] B. Higa, B.S. Cintra, C.M. Álvarez, A.B. Ribeiro, J.C. Ferreira, D.C. Tavares, et al., Ozonated oil is effective at killing *Candida* species and streptococcus mutans biofilm-derived cells under aerobic and microaerobic conditions, Med. Mycol. J. 60 (8) (2022), http://dx.doi.org/10.1093/mmy/myac055, myac055.

[29] E.I. Epelle, A. Emmerson, M. Nekrasova, A. Macfarlane, M. Cusack, A. Burns, et al., Microbial inactivation: gaseous or aqueous ozonation? Ind. Eng. Chem. Res. 61 (27) (2022) 9600–9610, http://dx.doi.org/10.1021/acs.iecr.2c01551.
[30] Z. Qiao, W. Zhang, H. Jiang, X. Li, W. An, H. Yang, 3D-printed composite scaffold with anti-infection and osteogenesis potential against infected bone defects, RSC Adv. 12 (18) (2022) 11008–11020, http://dx.doi.org/10.1039/D2RA00214K.
[31] Y. Feng, S. Chen, Z. Li, Z. Gu, S. Xu, X. Ban, et al., A review of controlled release from cyclodextrins: release methods release systems and application, Crit. Rev. Food Sci. Nutr. 63 (20) (2023) 4744–4756, http://dx.doi.org/10.1080/10408398.2021.2007352.
[32] D. Arora, A. Saneja, S. Jaglan, Cyclodextrin-based delivery systems for dietary pharmaceuticals, Environ. Chem. Lett. 17 (3) (2019) 1263–1270, http://dx.doi.org/10.1007/s10311-019-00878-w.
[33] B. Ramos-Martínez, C. Dávila-Pousa, V. Merino-Bohórquez, M.A. Marta García-Palomo, P. Flox-Benítez, Use of cyclodextrins as excipients in pharmaceutical products: why not in extemporaneous preparations? Farm. Hosp. 46 (1) (2022) 31–39, http://dx.doi.org/10.7399/fh.11728.
[34] J. Lee, S.S. Lee, S. Lee, H.B. Oh, Noncovalent complexes of cyclodextrin with small organic molecules: applications and insights into host–guest interactions in the gas phase and condensed phase, Molecules 25 (18) (2020) 4048, http://dx.doi.org/10.3390/molecules25184048.
[35] R.A. Rajewski, V.J. Stella, Pharmaceutical applications of cyclodextrins 2. In vivo drug delivery, J. Pharm. Sci. 85 (11) (1996) 1142–1169, http://dx.doi.org/10.1021/js960075u.
[36] M.I. Rodríguez-López, M.T. Mercader-Ros, S. López-Miranda, J.A. Pellicer, A. Pérez-Garrido, H. Pérez-Sánchez, et al., thorough characterization and stability of HP-β-cyclodextrin thymol inclusion complexes prepared by microwave technology: a required approach to a successful application in food industry, J. Sci. Food Agric. 99 (3) (2019) 1322–1333, http://dx.doi.org/10.1002/jsfa.9307.
[37] P. Saokham, C. Muankaew, P. Jansook, T. Loftsson, Solubility of cyclodextrins and drug/cyclodextrin complexes, Molecules 23 (5) (2018) 1161, http://dx.doi.org/10.3390/molecules23051161.
[38] D. Kida, B. Karolewicz, A. Junka, A. Sender-Janeczek, I. Duś, D. Marciniak, et al., Metronidazole-loaded porous matrices for local periodontitis treatment: in vitro evaluation and in vivo pilot study, Appl. Sci. 9 (21) (2019) 4545, http://dx.doi.org/10.3390/app9214545.
[39] S. Riela, G. Lazzara, P. Lo Meo, S. Guernelli, F. D'Anna, S. Milioto, et al., Microwave-assisted synthesis of novel cyclodextrin–cucurbituril complexes, Supramol. Chem. 23 (12) (2011) 819–828, http://dx.doi.org/10.1080/10610278.2011.636444.
[40] G. Al-Nasiri, M.J. Cran, A.J. Smallridge, S.W. Bigger, Optimisation of β-cyclodextrin inclusion complexes with natural antimicrobial agents: thymol, carvacrol and linalool, J. Microencapsul. 35 (1) (2018) 26–35, http://dx.doi.org/10.1080/02652048.2017.1413147.
[41] B. Prakash, A. Kujur, A. Yadav, A. Kumar, P.P. Singh, N.K. Dubey, Nanoencapsulation: an efficient technology to boost the antimicrobial potential of plant essential oils in food system, Food Control 89 (2018) 1–11, http://dx.doi.org/10.1016/j.foodcont.2018.01.018.
[42] C.I. Piñón-Balderrama, C. Leyva-Porras, Y. Terán-Figueroa, V. Espinosa-Solís, C. Álvarez-Salas, M.Z. Saavedra-Leos, Encapsulation of active ingredients in food industry by spray-drying and nano spray-drying technologies, Processes 8 (8) (2020) 889, http://dx.doi.org/10.1016/j.foodcont.2018.01.018.
[43] T.K. Higuchi, A. Connors, Phase-Solubility Techniques, 1965.
[44] M.I. Rodríguez-López, M.T. Mercader-Ros, A. Pérez-Garrido, H. Pérez-Sánchez, J.A. Pellicer, C. Lucas-Abellán, et al., Carvacrol and HP-β-cyclodextrin complexes: extensive characterization and potential cytotoxic effect in human colorectal carcinoma cells, Pharmaceutics 14 (12) (2022) 2638, http://dx.doi.org/10.3390/pharmaceutics14122638.
[45] B.K. Lee, J.H. Kim, J.W. Jung, J.W. Choi, E.S. Han, S.H. Lee, et al., Myristicin-induced neurotoxicity in human neuroblastoma SK-N-SH cells, Toxicol. Lett. 157 (1) (2005) 49–56, http://dx.doi.org/10.1016/j.toxlet.2005.01.012.
[46] C. Lucas-Abellán, M.I. Fortea, J.A. Gabaldón, E. Núñez-Delicado, Complexation of resveratrol by native and modified cyclodextrins: determination of complexation constant by enzymatic, solubility and fluorimetric assays, Food Chem. 111 (1) (2008) 262–267, http://dx.doi.org/10.1016/j.foodchem.2008.03.073.
[47] C.A. Di Battista, D. Constenla, M.V. Ramírez-Rigo, J. Piña, The use of arabic gum maltodextrin and surfactants in the microencapsulation of phytosterols by spray drying, Powder Technol. 286 (2015) 193–201, http://dx.doi.org/10.1016/j.powtec.2015.08.016.
[48] E.C. Frascareli, V.M. Silva, R.V. Tonon, M.D. Hubinger, Effect of process conditions on the microencapsulation of coffee oil by spray drying, Food Bioprod. Process. 90 (3) (2012) 413–424, http://dx.doi.org/10.1016/j.fbp.2011.12.002.
[49] L. De Bruyn, R. Coropciuc, W. Coucke, C. Politis, Microbial population changes in patients with medication-related osteonecrosis of the jaw treated with systemic antibiotics, Oral Surg. Oral Med. Oral Radiol. 125 (3) (2018) 268–275, http://dx.doi.org/10.1016/j.oooo.2017.11.022.
[50] F. Hallmer, T. Bjørnland, G. Andersson, J.P. Becktor, A.K. Kristoffersen, M. Enersen, Bacterial diversity in medication-related osteonecrosis of the jaw, Oral Surg. Oral Med. Oral Radiol. 123 (4) (2017) 436–444, http://dx.doi.org/10.1016/j.oooo.2016.11.011.
[51] M. Chierchia, S. Chirumbolo, L. Valdenassi, M. Franzini, Ozone-treated poly-ε-caprolactone scaffolds for bone regeneration, Chem.-Biol. Interact. 381 (2023) 110509, http://dx.doi.org/10.1016/j.cbi.2023.110509.
[52] S.S. Wong, P.C. Woo, W.K. Luk, K.Y. Yuen, Susceptibility testing of *Clostridium difficile* against metronidazole and vancomycin by disk diffusion and Etest, Diagn. Microbiol. Infect. Dis. 34 (1) (1999) 1–6, http://dx.doi.org/10.1016/S0732-8893(98)00139-4.